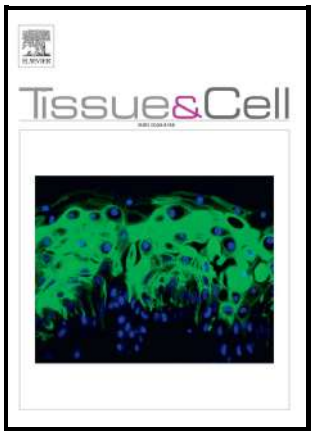

Enhancing Sciatic Nerve Regeneration with Osteopontin-Loaded Acellular Nerve Allografts in Rats: Effects on Macrophage Polarization

Shukur Wasman Smail, Shang Ziyad Abdulqadir, Lana Sardar Saleh Alalem, Taban Kamal Rasheed, Zhikal Omar Khudhur, Abdullah Faqiyazdin Ahmed Mzury, Harem Khdir Awla, Mohammad B. Ghayour, Arash Abdolmaleki

PII: S0040-8166(24)00080-6

DOI: https://doi.org/10.1016/j.tice.2024.102379

Reference: YTICE102379

To appear in: *Tissue and Cell*

Received date: 29 January 2024
Revised date: 5 April 2024
Accepted date: 9 April 2024

Please cite this article as: Shukur Wasman Smail, Shang Ziyad Abdulqadir, Lana Sardar Saleh Alalem, Taban Kamal Rasheed, Zhikal Omar Khudhur, Abdullah Faqiyazdin Ahmed Mzury, Harem Khdir Awla, Mohammad B. Ghayour and Arash Abdolmaleki, Enhancing Sciatic Nerve Regeneration with Osteopontin-Loaded Acellular Nerve Allografts in Rats: Effects on Macrophage Polarization, *Tissue and Cell,* (2024) doi:https://doi.org/10.1016/j.tice.2024.102379

Enhancing Sciatic Nerve Regeneration with Osteopontin-Loaded Acellular Nerve Allografts in Rats: Effects on Macrophage Polarization

Shukur Wasman Smail[1,2*], Shang Ziyad Abdulqadir[1], Lana Sardar Saleh Alalem[1], Taban Kamal Rasheed[1], Zhikal Omar Khudhur[3], Abdullah Faqiyazdin Ahmed Mzury[4,] Harem Khdir Awla[1], Mohammad B. Ghayour[5], Arash Abdolmaleki[6*]

[1] Department of Biology, College of Science, Salahaddin University- Erbil, Iraq

[2] Department of Medical Microbiology, College of Science, Cihan University-Erbil, Kurdistan Region, Iraq.

[3] Biology Education Department, Tishk International University, Erbil, Iraq.

[4] KBMS, College of Medicine, Hawler Medical University, Erbil, Kurdistan Region, Iraq.

[5] Department of Biology, Faculty of Science, Ferdowsi University of Mashhad, Mashhad, Iran.

[6] Department of Biophysics, Faculty of Advanced Technologies, University of Mohaghegh Ardabili, Namin, Iran.

Corresponding Authors: 1. Arash Abdolmaleki, Department of Biophysics, Faculty of Advanced Technologies, University of Mohaghegh Ardabili, Namin, Iran.

Tel: +989183705217 **E-mail:** Abdolmalekiarash1364@gmail.com

2. Shukur Wasman Smail 1. Department of Biology, College of Science, Salahaddin University-Erbil, Kurdistan Region, Iraq

Tel: +9647504491092 **E-mail:** shukur.smail@su.edu.krd

Abstract

Osteopontin (OPN) is a multifunctional matrix glycoprotein with neuroprotective and immunomodulatory properties. This study explored the potential of OPN-loaded acellular nerve allografts (ANAs) to repair sciatic nerves in male Wistar rats. The research also delved into the impact of OPN on macrophage phenotypes. We reconstructed a 10 mm nerve gap with ANAs containing OPN at 2 nM and 4 nM. The sciatic functional index (SFI) and paw withdrawal reflex latency (WRL) showed the significant efficacy of ANA/OPN (2 nM) in enhancement of target organ reinnervation and subsequent sensorimotor recovery compared to other groups. Electrophysiological and histomorphometric analyses further supported the regenerative properties of ANA/OPN (2 nM). Additionally, ANA/OPN (2 nM) promoted macrophage polarization towards an M2 phenotype and reduced proinflammatory cytokines at the injury site. In conclusion, the study suggested that ANA loaded with 2 nM OPN effectively repaired transected sciatic nerves in rats, potentially through enhancing axonal sprouting and exerting anti-inflammatory effects.

Keywords: Osteopontin, Acellular nerve allografts, Sciatic nerve, Macrophage, Rats

1. Introduction

Nerve autografting is the standard therapy for severe traumatic peripheral nerve injuries (PNIs) when end-to-end repair is not feasible. However, donor availability, size incompatibility, and neuroma formation limit the use of nerve autografts (Ray and Mackinnon, 2010). In this regard, acellular nerve allografts (ANAs) as tissue engineering scaffolds are attractive alternatives to nerve autografts. ANAs are derived from human tissue and provide a biocompatible three-dimensional scaffold for the growth of regenerating axons. They retain the native extracellular matrix (ECM) architecture and biochemical cues while minimizing immune responses due to reduced immunogenicity (Boriani et al., 2019). However, ANA efficacy is often lower than nerve autografts, especially for longer lesion gaps. In addition, ECM integrity loss, a lack of bioactive growth factors and biochemical guidance cues, insufficient mechanical strength, and vascularization deficits may reduce ANA regenerative efficacy (Peters et al., 2023; Thomson et al., 2022). Therefore, ongoing research is essential for enhancing the regenerative properties of decellularized scaffolds by incorporating growth factors, guidance cues, and vascularization strategies (Pedrini et al., 2019; Zheng et al., 2014). There is a growing interest in exploring the diverse functions of elements contributing to neuroinflammation and tissue remodeling, as they play a crucial role in achieving successful nerve regeneration. Evidence has shown that inflammation is vital for

nerve regeneration as it eliminates growth-inhibiting components and creates a supportive environment for axonal regrowth (Dubový et al., 2013; Stoll et al., 2002). Therefore, regulating the inflammatory response seems to be a suitable strategy for improving nerve regeneration.

In this regard, macrophages are essential for peripheral nerve regeneration and play a crucial role in the immune response and tissue repair following nerve injury (Niemi et al., 2013). Macrophages are categorized into pro-inflammatory (M1) and anti-inflammatory (M2) phenotypes, which serve different but equal functions in nerve regeneration. Following PNIs, there is an initial influx of pro-inflammatory macrophages within 3-7 days post-injury, followed by a transition to anti-inflammatory macrophages within 14-21 days post-injury, linked to tissue repair and regeneration (Mokarram et al., 2012). M1 macrophages secrete pro-inflammatory cytokines, phagocytose cellular debris, eliminate growth inhibitory factors, promote Schwann cell (SC) transdifferentiation, and create a conducive environment for axonal regeneration in the distal nerve (Chen et al., 2015; Niemi et al., 2013). Subsequently, M2 macrophages reduce initial inflammation, release trophic factors, enhance axon regrowth, and stimulate angiogenesis by releasing anti-inflammatory and pro-regenerative factors. M2 phenotype can also promote angiogenesis by releasing vascular endothelial growth factor (VEGF) (Liu et al., 2019). As a result, modulating the transition from M1 to M2 macrophages may enhance nerve regeneration by shifting the immune response to a more regenerative state, reducing inflammation, and promoting axonal growth and angiogenesis in damaged nerves.

In this regard, osteopontin (OPN) is a multifunctional glyco-phosphoprotein with both pro-inflammatory and anti-inflammatory properties, depending on the context (Lund et al., 2009). This dual functionality of OPN highlights its complex role in immune response modulation. OPN can act as a pro-inflammatory mediator by promoting the recruitment of immune cells, such as macrophages, to sites of inflammation and by increasing the production of pro-inflammatory mediators (Lund et al., 2009; Xu et al., 2023). Conversely, it can exert anti-inflammatory properties (Attur et al., 2001; Sun et al., 2024) by promoting macrophage polarization toward the M2 phenotype, suppressing pro-inflammatory cytokine synthesis, and enhancing anti-inflammatory cytokine release (Schuch et al., 2016). The versatile nature of OPN suggests its potential to shift the immune response towards a regenerative state, aiding tissue regeneration and contributing to the dynamic modulation of inflammation. Despite this,

the specific role of OPN in promoting peripheral nerve regeneration remains incompletely understood. This study aims to investigate the potential of OPN-loaded ANA for repairing sciatic nerve deficits in male Wistar rats, with a focus on understanding the modulatory effects of OPN on macrophages.

2- Material and Methods

2.1 Animals and Experimental Groups

The study employed male Wistar rats aged three months, weighing 215 ± 23 g. The rats were kept in plexiglass cages under standard lab conditions. The feeding and operation protocols for all animal experiments were carried out in accordance with the European Communities Council Directive of 24 November 1986(86/609/EEC) and approved by the Institutional Animal Care and Use Committee at Salahaddin University (Ethics No. 219 in 2023). The animals were allocated into healthy, sham-operated, autograft, ANA, ANA/vehicle, ANA/OPN (2 nM), and ANA/OPN (4 nM), with 18 animals in each group. Three days after surgery, four animals from each group were examined for cytokines. Another four animals from each group were randomly chosen to assess the macrophage phenotypes, 3 weeks post-surgery. Ten animals from each group were kept for behavioral, electrophysiological, and histological evaluations.

2.2 Preparation of ANA

As previously established by *Hudson* and her colleagues (Hudson et al., 2004), 15-mm sciatic nerve segments were harvested and submerged in distilled water for 7 hours under sterile conditions. The nerve specimens were treated with sulfobetaine-10 (SB-10) (Hopax, 15163-36-7) in phosphate-buffered sodium solution (PBS) for 15 hours. They were then submerged in PBS containing sulfobetaine-16 (SB-16) (Hopax, 2281-11-0) and Triton X-200 (Alfa Chemistry, ACM9010417-1) for 24 hours. After a wash with PBS, the specimens were immersed in a PBS solution with SB-10 for 7 hours, followed by rinsing in PBS and transferring to SB-16 and Triton X-200 solutions for 15 hours. The specimens were then stored in PBS at 4°C with 1% Penicillin/Streptomycin (Gibco, 15140122). 1% Toluidine blue (Sigma-Aldrich, 89640), Hematoxylin-Eosin (H&E) (Abcam, ab245880), and 4',6-diamidino-2-phenylindole (DAPI) (Abcam, ab228549) were used to confirm proper decellularization. Both ends of the decellularized nerves were trimmed to form a 10 mm graft, and recombinant rat OPN protein (R&D Systems, Cat. No. 6359-OP-050) in 20 µl PBS (0.67 µg/ml and 1.34

μg/ml) was injected by a Hamilton syringe with a 27-gauge needle into the acellular grafts from both ends. Once the injection was complete, the grafts were placed in a similar concentration of OPN solution and incubated for 24 hours.

2.3 Surgery

The experiment involved conducting aseptic surgeries on rats, wherein the animals were first anesthetized with a cocktail of ketamine (75 mg/kg; Alfasan) and xylazine (15 mg/kg; Alfasan) and then positioned on the side on a heating pad (37 °C). The left sciatic nerve was exposed, and a 10-mm-long piece was excited 1 cm above nerve trifurcation, leaving a gap that was filled with a 10-mm ANA and four epineural sutures (10-0 nylon, Ethicon). In the autograft group, 10 mm of the sciatic nerve was removed, reversed, and reinserted. The muscles and skin were then sutured, and the animals were allowed to recover from anesthesia. The sham-operated group underwent surgery without nerve damage (Bernal et al., 2009).

2.4 Walking Track Analysis

For assessment of motor recovery, the sciatic function index (SFI) was determined during walking track analysis preoperatively and on the 2nd, 4th, 8th, 12th, and 16th weeks post-operation. Rats with black ink-painted hind paws walked along a narrow runway, leaving footprints on white paper. The SFI was determined using the following formula: The SFI was then calculated as follows: SFI = -38.3 [(EPL-NPL)/NPL] + 109.5 [(ETS-NTS)/NTS] + 13.3 [(EIT-NIT)/NIT] - 8.8. In this formula, E and N refer to the injured and uninjured paws respectively. The paw length is represented by PL, the toe spread by TS, and the intermediary toe spread by IT. SFI values range from 0 (normal functioning) to -100 (complete impairment) (Sarikcioglu et al., 2009).

2.5 Thermal Nociception Assay

The thermal nociception threshold was evaluated with a Hargreaves apparatus (IITC Life Science Inc.) at the same time as the motor function test. Following acclimation, each rat was placed on a transparent glass surface with a 3-sided, allowing access to the hind paw. The hind paw was exposed to a radiant heat source at 54 ± 1 °C, and the duration from the onset of heat to paw withdrawal was measured as the paw withdrawal reflex latency (WRL). All

tests were conducted three times at 5-minute intervals, and the average results were recorded. A cut-off time of 20 seconds was established to avoid tissue damage. (Cheah et al., 2017).

2.6 Electrophysiological Evaluation

In the 16th week after surgery, compound muscle action potential (CMAP) and nerve conduction velocity (NCV) assessments were performed in isoflurane-anesthetized rats that were placed on a heating pad at 37 °C. We utilized a bipolar electrode to deliver electrical pulses upstream of the graft while recording and reference needle electrodes were placed into the muscle belly and Achilles tendon. Meanwhile, a ground electrode was inserted subdermally into the rat's tail. The nerve was excited sequentially with 0.2 ms supramaximal electrical pulses (10 mA) with an interstimulus interval of 400 ms to elicit the maximum CMAP amplitude. The CMAP was recorded at 10 kHz and then filtered using a high-pass filter at 1 kHz and a low-pass filter at 10 Hz. Additionally, the NCV was determined by dividing the distance between the stimulating and recording electrodes by the response latency (Schulz et al., 2014). The normal CMAP and NCV were recorded on the unaffected contralateral sciatic nerve. Finally, the rats were euthanized using CO2 inhalation.

2.7 Histomorphometry Analysis

As previously described, a histomorphometry assessment was done to evaluate the regenerated sciatic nerves in rats. Following euthanasia, 5 mm nerve segments were harvested 5 mm downstream from the grafts, fixed in 4% paraformaldehyde (PFA) and 3% glutaraldehyde solution, dehydrated in an ethanol series, and embedded in resin. Subsequently, the 1μm-thick toluidine blue-stained sections were captured by Carl Zeiss light microscopy (Germany) (Scipio et al., 2008). Finally, a blinded observer manually counted the total number of myelinated fibers in each full cross-section of a nerve section. The counts were estimated from a systematic random sampling of fields representing 20% of the cross-sectional area. The counted fields were analyzed using ImageJ 2.0.0 software (National Institutes of Health). In addition to the fiber counts, the diameter of the myelinated fibers, axons, and the myelin thickness were manually measured in the sampled fields (Geuna et al., 2001). The unaffected contralateral nerve was used as a control.

2.8 Immunofluorescence Staining

Three weeks post-surgery, the macrophage M1/M2 ratio in the implanted grafts was measured using immunostaining. Following transcardial perfusion with 4% PFA, the nerve grafts were collected, post-fixed in 4% PFA, and embedded in the TissueTek O.C.T. compound (Sakura). The 10 µm cryo-sectioned nerves were treated with 10% fetal bovine serum (FBS; Gibco) for blocking, and then incubated overnight at 4˚C with primary antibodies, including rat anti-mouse CD68 monoclonal antibody (1:100, IgG2a, Bio-Rad, MCA1957), rat anti-mouse CCR7 monoclonal antibody (1:100, IgG2a, R&D Systems, MAB3477), and rat anti-mouse CD206 monoclonal antibody (1:100, IgG2a, Bio-Rad, MCA2235). The specimens were then washed with a PBS-triton 0.5% solution and immersed in a secondary antibody solution with triton X100 0.5% for one hour at the laboratory temperature. Secondary antibodies, Alexa Fluor 594 (red) mouse anti-rat IgG2a (1:200, Biolegend, 407509) and Alexa Fluor 488 (green) mouse anti-rat IgG2a (1:200, Biolegend, 407514), were applied at a 1:500 dilution (Isidro et al., 2015). Subsequently, the stained nerve sections were washed with PBS, covered with a slip, and observed under a fluorescence microscope (Axioskop 2, Zeiss). The ratio of macrophages was calculated by analyzing one image per animal, using the whole cross-sectional area for quantification.

2.9 Cytokine Assay

Three days post-operatively, a sandwich Enzyme-Linked Immunosorbent Assay (ELISA) measured interleukin-1β (IL-1β), Tumor necrosis factor-α (TNF-α), interleukin-4 (IL-4), interleukin-10 (IL-10) in the implanted grafts. The nerve samples were first homogenized in radioimmunoprecipitation assay buffer (RIPA buffer) with protease inhibitors, and the protein concentration was measured by a Bicinchoninic Acid (BCA) Protein Assay reagent kit (Abcam; ab102536). After centrifuging the nerve homogenate for 30 minutes at 15,000 x g, the supernatant was collected, and cytokine concentrations were assessed with the Rat IL-1β ELISA Kit (ab100768; Abcam), Rat IL-4 ELISA Kit (ab100771; Abcam), Rat IL-10 ELISA Kit (ab100765; Abcam), and Rat TNF-α ELISA Kit (ab100785; Abcam) following the manufacturer's protocols. The optical density (OD) was determined by a colorimetric assay at 450 nm after adding 100 µL of stop solution to each sample. Finally, the cytokine content was estimated by a standard curve created by known concentrations of recombinant cytokines.

2.10 Statistical Analysis

SPSS Statistics 20.0 (SPSS Inc., Chicago, Illinois, USA) was used to analyze the data. The normality of the data was determined using the Kolmogorov-Smirnoff test. Multiple group comparisons were performed by one-way analysis of variance (ANOVA). A Tukey-post hoc analysis was conducted to compare the two groups. Results were considered statistically significant if $P < 0.05$. The data are shown as mean ± Standard Error of Mean (SEM).

3. Results

This research evaluated the effectiveness of ANA loaded with OPN in repairing rat sciatic nerve gaps. Histological analysis confirmed the successful removal of cells, axons, and myelin from decellularized nerves while preserving the ECM architecture, which has been described elsewhere (Omar Khudhur et al., 2023). Except for one animal from the ANA group and two animals from the ANA/OPN (4 nM) groups that were euthanized with CO asphyxiation due to autotomy, other animals survived without complications. To simplify, data from the healthy and ANA/vehicle groups were not presented due to the lack of significant differences compared to sham-operated and ANA groups.

3.1. Sensory-Motor Function Recovery

The motor function and thermal nociception were assessed using SFI and hind paw WRL. Before the surgery, all animals had normal motor and sensory functions. However, in the second-week post-surgery, they experienced severe motor weakness (Fig. 1A) and sensory numbness (Fig. 1B) in the left hind paw, except for those without nerve damage. Afterward, the regenerative responses were observed, and over time, all animals with sciatic nerve deficits showed progressive target organ reinnervation, as indicated by improving SFI and WRL values at different rates. As shown in Figures 1A and 1B, reconstructing nerves with ANA/OPN (2 nM) led to statistically significant improvements in SFI and WRL at all measurement times after the second postoperative week in comparison with the ANA and ANA/OPN (4 nM) groups ($P < 0.01$). However, while the improvement in SFI and WRL parameters did not differ significantly between the ANA/OPN (2 nM) and autograft groups in the early postoperative weeks, the autograft group was significantly superior in the later weeks ($P < 0.05$). Furthermore, the ANA/OPN (4 nM) group recovered better than the ANA group in the 8th, 12th, and 16th postoperative weeks in motor function and the 12th and 16th weeks in sensory function ($P < 0.05$). Overall, the results of the sensorimotor assessment revealed that the Autograft and the ANA/OPN (2 nM) groups had relatively better functional

recovery compared to the ANA and ANA/OPN (4 nM) groups, especially at the later time points.

3.2. Electrophysiological Assessment

Electrophysiological assessment at the end of the 16th week enumerated CMAP amplitude and NCV in nerve-reconstructed legs. According to the results, the ANA/OPN (2 nM) group exhibited significant improvements in comparison with the ANA and ANA/OPN (4 nM) groups in terms of CMAP amplitudes (Fig. 2A; $P < 0.01$) and NCV values (Fig. 2B; $P < 0.001$). In both parameters, the ANA/OPN (4 nM) group outperformed the ANA groups ($P < 0.05$). Furthermore, the CMAP amplitudes and NCV values in the ANA/OPN (2 nM) group were meaningfully lower than those in the autograft group ($P < 0.01$).

3.3. Histomorphometry

Table 1 revealed a morphometric assessment of sciatic nerves, and toluidine blue staining was performed to compare axon regrowth and remyelination between groups (Fig. 3). The results demonstrated that the myelinated fiber number, fiber diameter, and myelin thickness in the ANA/OPN (2 nM) recipient rats were significantly higher than those in the ANA and ANA/OPN (4 nM) groups, with statistical significance ($P < 0.05$). In all parameters, the ANA/OPN (4 nM) group outperformed the ANA groups ($P < 0.05$), as the autograft group was superior to the ANA/OPN (2 nM) ($P < 0.001$). In addition, the highest number of myelinated fibers in the distal nerve segment was observed in the autograft, ANA/OPN (2 nM), and ANA/OPN (4 nM) groups, respectively. These findings highlight the potential of OPN treatment for enhancing nerve regeneration as well as the dose-dependent nature of its effects on histomorphometric outcomes.

3.4. Macrophage Phenotype

Three weeks post-surgery, the ratio of CD68+CCR7+ (M1) macrophages as an inflammatory phenotype to the CD68+CD206+ (M2) macrophage as a pro-healing phenotype was quantified using an immunostaining technique. Although CD68+CCR7+ macrophages (Fig. 4A) and CD68+CD206+ macrophages (Fig. 4B) were observed in any group, the ANA/OPN (4 nM) group had the higher ratio of CD68+CCR7+ macrophages ($P < 0.001$) and the ANA/OPN (2 nM) group had the highest percentage of CD68+CD206+ macrophages ($P < 0.001$) when compared to other groups ($P < 0.01$). In autograft recipient rats, we found that

the CD68+CD206+ macrophage percentage (Fig. 4) was higher than in those receiving ANA ($P < 0.01$).

3.5. ELISA Assay

The results of the ELISA assay are also shown in Figure 5. The findings indicated a significant decrease in the IL-1β (Fig. 5A) and TNF-α (Fig. 5B) concentrations and an increase in the IL-4 (Fig. 5C) and IL-10 (Fig. 5D) levels in rats that received ANA/OPN (2 nM) compared to those that received ANA/OPN (4 nM) grafts ($P < 0.05$). However, in comparison to the autograft group, the IL-4 and IL-10 levels were significantly lower in the ANA/OPN (2 nM) group, while no significant difference was observed in terms of IL-1β and TNF-α levels. Conversely, the highest concentration of IL-1β and TNF-α was observed in ANA/OPN (4 nM) recipient rats (Fig. 5; $P < 0.05$). This was while the level of IL-4 and IL-10 in these animals was inferior to the autograft group ($P < 0.05$). While the autograft group also had higher levels of IL-4 and IL-10, the concentration of all four cytokines in the ANA group was lower than the others.

4. Discussion

PNIs are a common clinical issue worldwide, and they account for around 2–3% of all trauma cases (Padovano et al., 2022). Severe nerve lesions often lead to inadequate healing when the nerve gap is long and end-to-end neurorrhaphy is not feasible. Nerve autografting is currently the gold standard for severe nerve defect reconstruction (Ray and Mackinnon, 2010). ANA is gaining attention as an alternative to nerve autografts due to the latter's limitations (Hudson et al., 2004). Although cadaveric nerve allografts are valuable for repairing nerves, their effectiveness decreases for severe defects (Pedrini et al., 2019). Enhancing the regenerative potential of ANAs can be achieved by refining decellularization methods, incorporating bioactive substances and neurotrophic factors, and regulating the immune reaction.

In this regard, we suppose that OPN addition to decellularized nerves improves the scaffold's regenerative capabilities by modulating the immune response and facilitating the regeneration of axons. OPN is a multifunctional extracellular matrix protein, encoded by the SPP1 gene in humans, implicated in various physiological processes and pathological conditions, such as bone formation (Morinobu et al., 2003), inflammation (Lund et al., 2009), stress responses (Wang and Denhardt, 2008), and cancer (Shevde and Samant, 2014). Recently, OPN has also emerged as a neuronal survival and regeneration modulator (Meller et al., 2005). It can be

found in various nervous system cells, including neurons(Marsh et al., 2007), astrocytes (Albertsson et al., 2014), microglia (Rosmus et al., 2022), and SCs (Ahn et al., 2004). OPN has been shown to promote neural regeneration following central nervous system (CNS) injury. For example, OPN administration has been shown to protect neurons from apoptosis and promote axonal regeneration following spinal cord injury (Fu et al., 2004). It can also regulate the behavior of glial cells, such as astrocytes and microglia, which are critical in CNS regeneration (Albertsson et al., 2014; Rosmus et al., 2022). In the PNS, OPN has been associated with promoting axon regeneration, regulating the immune response, promoting SC proliferation and differentiation, and enhancing axon regeneration following PNIs (Duan et al., 2015; Wright et al., 2014). It influences macrophage polarization, promoting the transition from the pro-inflammatory M1 to the pre-healing M2 phenotype, possibly enhancing nerve regeneration (Liu et al., 2019). M1 macrophages trigger inflammation to clear cell debris, but excessive presence can harm regeneration. M2 macrophages promote axonal regeneration and create a favorable environment for nerve regeneration (Mokarram et al., 2012). As the repair process progresses, the delicate balance between M1 and M2 macrophages becomes the linchpin of success (Huang et al., 2020). OPN can inhibit apoptosis by binding to and activating the death receptor Fas. OPN can also promote angiogenesis, which is significant for tissue regeneration (Dai et al., 2009). The neuroprotective effects of OPN have led to the development of some OPN-based therapies for neurodegenerative diseases and spinal cord injuries (Cappellano et al., 2021; Rentsendorj et al., 2018; Wang et al., 2023). Accordingly, this research used a rat model of sciatic nerve injury to assess the regeneration capacity of ANA-loaded OPN. We exposed regenerated axons to OPN locally by loading it into ANA, potentially reducing systemic adverse effects.

Our results revealed significant improvements in sensory-motor function recovery in sciatic nerves reconstructed with ANA/OPN (2 nM) and ANA/OPN (4 nM) compared to those given ANA. Electrophysiological assessments confirmed behavioral findings, with both the ANA/OPN (2 nM) and ANA/OPN (4 nM) groups showing significant improvements in CMAP amplitudes and NCV values compared to the ANA group. Histomorphometry analysis revealed that ANA/OPN (2 nM) had superior regenerative potential compared to ANA and ANA/OPN (4 nM) and enhanced nerve regeneration. Overall, ANA/OPN treatment, particularly at 2 nM concentration, holds promise for improving sensory-motor function recovery following nerve injury and could have implications for regenerative medicine. The analysis of macrophage polarization revealed considerable distinctions between the groups.

Three weeks after nerve repair, the ANA/OPN (4 nM) group showcased a higher percentage of CD68+CCR7+ macrophages, while the ANA/OPN (2 nM) group displayed the highest ratio of CD68+CD206+ macrophages. In addition, the ELISA assay demonstrated that the ANA/OPN (2 nM) treatment caused a statistical decline in pro-inflammatory cytokines (IL-1β and TNF-α) and a rise in anti-inflammatory cytokines (IL-4 and IL-10), while ANA/OPN (4 nM) exhibited the highest level of pro-inflammatory cytokines. The choice of measuring the phenotype of macrophages and the concentration of inflammatory cytokines three weeks after nerve damage is well justified due to the critical events occurring during this timeframe. Two to three weeks post-nerve damage marks a pivotal stage characterized by the completion of Wallerian degeneration and the initiation of axonal growth, signifying the transition from the inflammatory phase to the repair phase (Chen et al., 2015). This transition is crucial as it signifies the shift in macrophage phenotype from pro-inflammatory (M1) to pro-healing (M2), which plays a central role in promoting the nerve repair process. Additionally, at this stage, the microenvironment within the injured nerve is likely to exhibit a dynamic balance of pro-inflammatory and pro-regenerative signals, making it an optimal time point for assessing the impact of macrophage phenotype and cytokine concentrations on nerve repair. This period also aligns with the onset of axonal regeneration, making it a critical window for evaluating the interplay between inflammation, macrophage phenotype, and nerve repair outcomes (Mokarram et al., 2012; Zigmond and Echevarria, 2019). In this regard, our findings suggest that OPN at a concentration of 2 nM has enhancing effects on macrophage polarization toward a pro-healing phenotype and anti-inflammatory cytokine levels, indicating its potential for modulating the immune response and promoting neurotrophic support in nerve regeneration.

Previous studies have highlighted the significance of targeting the OPN for neural regeneration. In this regard, Jander and colleagues studied the expression of OPN in rat sciatic nerves during Wallerian degeneration. They found that axon signals controlled OPN expression in SCs. After axotomy, OPN expression in SCs briefly increased in the distal nerve stump before decreasing to its lowest level on the 14th-day post-injury. However, regenerating nerves showed re-expression of OPN in SCs (Jander et al., 2002). In another study, Wright and colleagues found that OPN increased in denervated motor axons in transected sciatic nerve. OPN mRNA expression increased significantly seven days after transection and OPN protein expression peaked between 14 and 30 days. Loss of OPN led to lower motor regeneration in mice, while exogenously administered OPN stimulated the

expansion of cultured motor neurons (Wright et al., 2014). In 2004, Ahn and colleagues studied the OPN expression in a rat experimental autoimmune neuritis (EAN). They found that OPN expression was amplified in the SCs of sciatic nerves and remained high even after recovery from leg paralysis, suggesting that it has an immunostimulatory effect and can magnify the inflammatory response (Ahn et al., 2004).

Other studies suggest that OPN has controversial effects on various health conditions. In chronic inflammatory diseases such as autoimmune disorders (Agnholt et al., 2007; Hur et al., 2007; Orsi et al., 2021; Xu et al., 2022), autoimmune encephalitis (Clemente et al., 2017; Zou et al., 2020), cancer (Bandopadhyay et al., 2014; Rittling and Chambers, 2004), and liver disorders (Leung et al., 2013; Song et al., 2021), OPN plays a proinflammatory role. However, it suppresses inducible nitric oxide synthase (iNOS) and aids phagocytosis to promote wound healing in diseases like traumatic brain injuries (TBIs), which are significantly associated with macrophage or microglia function (Gao et al., 2020; Scatena et al., 2007; Schroeter et al., 2006). Some studies have also reported anti-inflammatory and microglia modulatory effects of OPNs in cerebral ischemia (Ladwig et al., 2017) and intracerebral hemorrhage (Gong et al., 2018) models. After cerebral infarction, OPN expression increases in microglia and macrophages, which promotes the migration of macrophages and astrocytes to the infarction site. OPN has neuroprotective effects and can reduce inflammation by enhancing microglia polarization towards the M2 phenotype and increasing the secretion of anti-inflammatory cytokines. The integrin-FAK-STAT3 and nuclear factor kappa B (NF-κB) signaling pathways facilitate neuroprotection (Sun et al., 2024). Some studies have also revealed an increase in OPN expression following spinal cord injury.

5. Conclusion

We aimed to investigate the use of ANA loaded with OPN for reconstructing peripheral nerve gaps in a rat model. Our findings indicate that low concentrations of OPN enhance ANA's regenerative properties, leading to efficient nerve regeneration and better sensorimotor recovery. We observed that OPN treatment significantly polarizes macrophages toward the M2 phenotype and attenuates the pro-inflammatory response in the sciatic nerve.

Limitations

Although ANA/OPN treatment has shown promising results in enhancing sensory-motor function recovery and nerve regeneration after injury, the present study has some limitations. It mainly focused on short-term outcomes and the long-term effects of the treatment need to be studied. Also, the mechanisms underlying the observed improvements are not fully understood, and further research is needed to investigate the optimal dosage and timing of OPN administration. Comprehensive long-term studies and mechanistic investigations are needed to validate and translate the findings of this study into clinical applications in regenerative medicine.

Acknowledgments

This research is funded by the University of Mohaghegh Ardabili, Iran, and Tishk International University in Erbil, Kurdistan Region, Iraq. We express our gratitude for their support.

Conflict Of Interest

The authors do not have any conflicts of interest to disclose.

References

Agnholt, J., Kelsen, J., Schack, L., Hvas, C., Dahlerup, J., Sørensen, E., 2007. Osteopontin, a protein with cytokine-like properties, is associated with inflammation in Crohn's disease. Scandinavian journal of immunology 65, 453-460.

Ahn, M., Lee, Y., Moon, C., Jin, J.-K., Matsumoto, Y., Koh, C.-S., Kim, H.-M., Shin, T., 2004. Upregulation of osteopontin in Schwann cells of the sciatic nerves of Lewis rats with experimental autoimmune neuritis. Neuroscience letters 372, 137-141.

Albertsson, A.-M., Zhang, X., Leavenworth, J., Bi, D., Nair, S., Qiao, L., Hagberg, H., Mallard, C., Cantor, H., Wang, X., 2014. The effect of osteopontin and osteopontin-derived peptides on preterm brain injury. Journal of neuroinflammation 11, 1-13.

Attur, M.G., Dave, M.N., Stuchin, S., Kowalski, A.J., Steiner, G., Abramson, S.B., Denhardt, D.T., Amin, A.R., 2001. Osteopontin: an intrinsic inhibitor of inflammation in cartilage. Arthritis & Rheumatism 44, 578-584.

Bandopadhyay, M., Bulbule, A., Butti, R., Chakraborty, G., Ghorpade, P., Ghosh, P., Gorain, M., Kale, S., Kumar, D., Kumar, S., 2014. Osteopontin as a therapeutic target for cancer. Expert opinion on therapeutic targets 18, 883-895.

Bernal, J., Baldwin, M., Gleason, T., Kuhlman, S., Moore, G., Talcott, M., 2009. Guidelines for rodent survival surgery. Journal of Investigative Surgery 22, 445-451.

Boriani, F., Fazio, N., Bolognesi, F., Pedrini, F.A., Marchetti, C., Baldini, N., 2019. Noncellular modification of acellular nerve allografts for peripheral nerve reconstruction: a systematic critical review of the animal literature. World neurosurgery 122, 692-703. e692.

Cappellano, G., Vecchio, D., Magistrelli, L., Clemente, N., Raineri, D., Mazzucca, C.B., Virgilio, E., Dianzani, U., Chiocchetti, A., Comi, C., 2021. The Yin-Yang of osteopontin in nervous system diseases: damage versus repair. Neural regeneration research 16, 1131.

Cheah, M., Fawcett, J.W., Andrews, M.R., 2017. Assessment of thermal pain sensation in rats and mice using the Hargreaves test. Bio-protocol 7, e2506-e2506.

Chen, P., Piao, X., Bonaldo, P., 2015. Role of macrophages in Wallerian degeneration and axonal regeneration after peripheral nerve injury. Acta neuropathologica 130, 605-618.
Clemente, N., Comi, C., Raineri, D., Cappellano, G., Vecchio, D., Orilieri, E., Gigliotti, C.L., Boggio, E., Dianzani, C., Sorosina, M., 2017. Role of anti-osteopontin antibodies in multiple sclerosis and experimental autoimmune encephalomyelitis. Frontiers in immunology 8, 321.
Dai, J., Peng, L., Fan, K., Wang, H., Wei, R., Ji, G., Cai, J., Lu, B., Li, B., Zhang, D., 2009. Osteopontin induces angiogenesis through activation of PI3K/AKT and ERK1/2 in endothelial cells. Oncogene 28, 3412-3422.
Duan, X., Qiao, M., Bei, F., Kim, I.-J., He, Z., Sanes, J.R., 2015. Subtype-specific regeneration of retinal ganglion cells following axotomy: effects of osteopontin and mTOR signaling. Neuron 85, 1244-1256.
Dubový, P., Jančálek, R., Kubek, T., 2013. Role of inflammation and cytokines in peripheral nerve regeneration. International review of neurobiology 108, 173-206.
Fu, Y., Hashimoto, M., Ino, H., Murakami, M., Yamazaki, M., Moriya, H., 2004. Spinal root avulsion-induced upregulation of osteopontin expression in the adult rat spinal cord. Acta neuropathologica 107, 8-16.
Gao, N., Zhang-Brotzge, X., Wali, B., Sayeed, I., Chern, J.J., Blackwell, L.S., Kuan, C.-Y., Reisner, A., 2020. Plasma osteopontin may predict neuroinflammation and the severity of pediatric traumatic brain injury. Journal of Cerebral Blood Flow & Metabolism 40, 35-43.
Geuna, S., Tos, P., Guglielmone, R., Battiston, B., Giacobini-Robecchi, M.G., 2001. Methodological issues in size estimation of myelinated nerve fibers in peripheral nerves. Anatomy and embryology 204, 1-10.
Gong, L., Manaenko, A., Fan, R., Huang, L., Enkhjargal, B., McBride, D., Ding, Y., Tang, J., Xiao, X., Zhang, J.H., 2018. Osteopontin attenuates inflammation via JAK2/STAT1 pathway in hyperglycemic rats after intracerebral hemorrhage. Neuropharmacology 138, 160-169.
Huang, T.-C., Wu, H.-L., Chen, S.-H., Wang, Y.-T., Wu, C.-C., 2020. Thrombomodulin facilitates peripheral nerve regeneration through regulating M1/M2 switching. Journal of neuroinflammation 17, 1-14.
Hudson, T.W., Liu, S.Y., Schmidt, C.E., 2004. Engineering an improved acellular nerve graft via optimized chemical processing. Tissue engineering 10, 1346-1358.
Hur, E.M., Youssef, S., Haws, M.E., Zhang, S.Y., Sobel, R.A., Steinman, L., 2007. Osteopontin-induced relapse and progression of autoimmune brain disease through enhanced survival of activated T cells. Nature immunology 8, 74-83.
Isidro, R.A., Isidro, A.A., Cruz, M.L., Hernandez, S., Appleyard, C.B., 2015. Double immunofluorescent staining of rat macrophages in formalin-fixed paraffin-embedded tissue using two monoclonal mouse antibodies. Histochemistry and cell biology 144, 613-621.
Jander, S., Bussini, S., Neuen-Jacob, E., Bosse, F., Menge, T., Müller, H.W., Stoll, G., 2002. Osteopontin: a novel axon-regulated Schwann cell gene. Journal of neuroscience research 67, 156-166.
Ladwig, A., Walter, H.L., Hucklenbroich, J., Willuweit, A., Langen, K.-J., Fink, G.R., Rueger, M.A., Schroeter, M., 2017. Osteopontin augments M2 microglia response and separates M1-and M2-polarized microglial activation in permanent focal cerebral ischemia. Mediators of inflammation 2017.
Leung, T.-M., Wang, X., Kitamura, N., Fiel, M.I., Nieto, N., 2013. Osteopontin delays resolution of liver fibrosis. Laboratory investigation 93, 1082-1089.
Liu, P., Peng, J., Han, G.-H., Ding, X., Wei, S., Gao, G., Huang, K., Chang, F., Wang, Y., 2019. Role of macrophages in peripheral nerve injury and repair. Neural regeneration research 14, 1335.
Lund, S.A., Giachelli, C.M., Scatena, M., 2009. The role of osteopontin in inflammatory processes. Journal of cell communication and signaling 3, 311-322.
Marsh, B.C., Kerr, N.C., Isles, N., Denhardt, D.T., Wynick, D., 2007. Osteopontin expression and function within the dorsal root ganglion. Neuroreport 18, 153.
Meller, R., Stevens, S.L., Minami, M., Cameron, J.A., King, S., Rosenzweig, H., Doyle, K., Lessov, N.S., Simon, R.P., Stenzel-Poore, M.P., 2005. Neuroprotection by osteopontin in stroke. Journal of Cerebral Blood Flow & Metabolism 25, 217-225.

Mokarram, N., Merchant, A., Mukhatyar, V., Patel, G., Bellamkonda, R.V., 2012. Effect of modulating macrophage phenotype on peripheral nerve repair. Biomaterials 33, 8793-8801.
Morinobu, M., Ishijima, M., Rittling, S.R., Tsuji, K., Yamamoto, H., Nifuji, A., Denhardt, D.T., Noda, M., 2003. Osteopontin expression in osteoblasts and osteocytes during bone formation under mechanical stress in the calvarial suture in vivo. Journal of Bone and Mineral Research 18, 1706-1715.
Niemi, J.P., DeFrancesco-Lisowitz, A., Roldán-Hernández, L., Lindborg, J.A., Mandell, D., Zigmond, R.E., 2013. A critical role for macrophages near axotomized neuronal cell bodies in stimulating nerve regeneration. Journal of Neuroscience 33, 16236-16248.
Omar Khudhur, Z., Ziyad Abdulqadir, S., Faqiyazdin Ahmed Mzury, A., Aziz Rasoul, A., Wasman Smail, S., Ghayour, M.B., Abdolmaleki, A., 2023. Epothilone B loaded in acellular nerve allograft enhanced sciatic nerve regeneration in rats. Fundamental & Clinical Pharmacology.
Orsi, G., Hayden, Z., Cseh, T., Berki, T., Illes, Z., 2021. Osteopontin levels are associated with late-time lower regional brain volumes in multiple sclerosis. Scientific Reports 11, 23604.
Padovano, W.M., Dengler, J., Patterson, M.M., Yee, A., Snyder-Warwick, A.K., Wood, M.D., Moore, A.M., Mackinnon, S.E., 2022. Incidence of nerve injury after extremity trauma in the United States. Hand 17, 615-623.
Pedrini, F.A., Boriani, F., Bolognesi, F., Fazio, N., Marchetti, C., Baldini, N., 2019. Cell-enhanced acellular nerve allografts for peripheral nerve reconstruction: a systematic review and a meta-analysis of the literature. Neurosurgery 85, 575-604.
Peters, B.R., Wood, M.D., Hunter, D.A., Mackinnon, S.E., 2023. Acellular nerve allografts in major peripheral nerve repairs: An analysis of cases presenting with limited recovery. Hand 18, 236-243.
Ray, W.Z., Mackinnon, S.E., 2010. Management of nerve gaps: autografts, allografts, nerve transfers, and end-to-side neurorrhaphy. Experimental Neurology 223, 77-85.
Rentsendorj, A., Sheyn, J., Fuchs, D.-T., Daley, D., Salumbides, B.C., Schubloom, H.E., Hart, N.J., Li, S., Hayden, E.Y., Teplow, D.B., 2018. A novel role for osteopontin in macrophage-mediated amyloid-β clearance in Alzheimer's models. Brain, behavior, and immunity 67, 163-180.
Rittling, S., Chambers, A., 2004. Role of osteopontin in tumour progression. British journal of cancer 90, 1877-1881.
Rosmus, D.-D., Lange, C., Ludwig, F., Ajami, B., Wieghofer, P., 2022. The role of osteopontin in microglia biology: Current concepts and future perspectives. Biomedicines 10, 840.
Sarikcioglu, L., Demirel, B., Utuk, A., 2009. Walking track analysis: an assessment method for functional recovery after sciatic nerve injury in the rat. Folia morphologica 68, 1-7.
Scatena, M., Liaw, L., Giachelli, C.M., 2007. Osteopontin: a multifunctional molecule regulating chronic inflammation and vascular disease. Arteriosclerosis, thrombosis, and vascular biology 27, 2302-2309.
Schroeter, M., Zickler, P., Denhardt, D.T., Hartung, H.-P., Jander, S., 2006. Increased thalamic neurodegeneration following ischaemic cortical stroke in osteopontin-deficient mice. Brain 129, 1426-1437.
Schuch, K., Wanko, B., Ambroz, K., Castelo-Rosa, A., Moreno-Viedma, V., Grün, N.G., Leitner, L., Staffler, G., Zeyda, M., Stulnig, T.M., 2016. Osteopontin affects macrophage polarization promoting endocytic but not inflammatory properties. Obesity 24, 1489-1498.
Schulz, A., Walther, C., Morrison, H., Bauer, R., 2014. In vivo electrophysiological measurements on mouse sciatic nerves. JoVE (Journal of Visualized Experiments), e51181.
Scipio, F.D., Raimondo, S., Tos, P., Geuna, S., 2008. A simple protocol for paraffin-embedded myelin sheath staining with osmium tetroxide for light microscope observation. Microscopy research and technique 71, 497-502.
Shevde, L.A., Samant, R.S., 2014. Role of osteopontin in the pathophysiology of cancer. Matrix Biology 37, 131-141.
Song, Z., Chen, W., Athavale, D., Ge, X., Desert, R., Das, S., Han, H., Nieto, N., 2021. Osteopontin takes center stage in chronic liver disease. Hepatology 73, 1594-1608.
Stoll, G., Jander, S., Myers, R.R., 2002. Degeneration and regeneration of the peripheral nervous system: from Augustus Waller's observations to neuroinflammation. Journal of the Peripheral Nervous System 7, 13-27.

Sun, C., Rahman, M.S.U., Enkhjargal, B., Peng, J., Zhou, K., Xie, Z., Wu, L., Zhang, T., Zhu, Q., Tang, J., 2024. Osteopontin modulates microglial activation states and attenuates inflammatory responses after subarachnoid hemorrhage in rats. Experimental Neurology 371, 114585.
Thomson, C., Schneider, J.M., Pohl, U., Power, D.M., 2022. Failed acellular nerve allografts: a critical review. Annals of plastic surgery 89, 63-71.
Wang, K.X., Denhardt, D.T., 2008. Osteopontin: role in immune regulation and stress responses. Cytokine & growth factor reviews 19, 333-345.
Wang, Y., Su, H., Zhong, J., Zhan, Z., Zhao, Q., Liu, Y., Li, S., Wang, H., Yang, C., Yu, L., 2023. Osteopontin enhances the effect of treadmill training and promotes functional recovery after spinal cord injury. Molecular Biomedicine 4, 44.
Wright, M.C., Mi, R., Connor, E., Reed, N., Vyas, A., Alspalter, M., Coppola, G., Geschwind, D.H., Brushart, T.M., Höke, A., 2014. Novel roles for osteopontin and clusterin in peripheral motor and sensory axon regeneration. Journal of Neuroscience 34, 1689-1700.
Xu, C., Wu, Y., Liu, N., 2022. Osteopontin in autoimmune disorders: Current knowledge and future perspective. Inflammopharmacology 30, 385-396.
Xu, Z., Xi, F., Deng, X., Ni, Y., Pu, C., Wang, D., Lou, W., Zeng, X., Su, N., Chen, C., 2023. Osteopontin promotes macrophage M1 polarization by activation of the JAK1/STAT1/HMGB1 signaling pathway in nonalcoholic fatty liver disease. Journal of Clinical and Translational Hepatology 11, 273.
Zheng, C., Zhu, Q., Liu, X., Huang, X., He, C., Jiang, L., Quan, D., 2014. Improved peripheral nerve regeneration using acellular nerve allografts loaded with platelet-rich plasma. Tissue Engineering Part A 20, 3228-3240.
Zigmond, R.E., Echevarria, F.D., 2019. Macrophage biology in the peripheral nervous system after injury. Progress in neurobiology 173, 102-121.
Zou, C., Pei, S., Yan, W., Lu, Q., Zhong, X., Chen, Q., Pan, S., Wang, Z., Wang, H., Zheng, D., 2020. Cerebrospinal fluid Osteopontin and inflammation-associated cytokines in patients with anti-N-methyl-D-aspartate receptor encephalitis. Frontiers in Neurology 11, 519692.

Figure legends

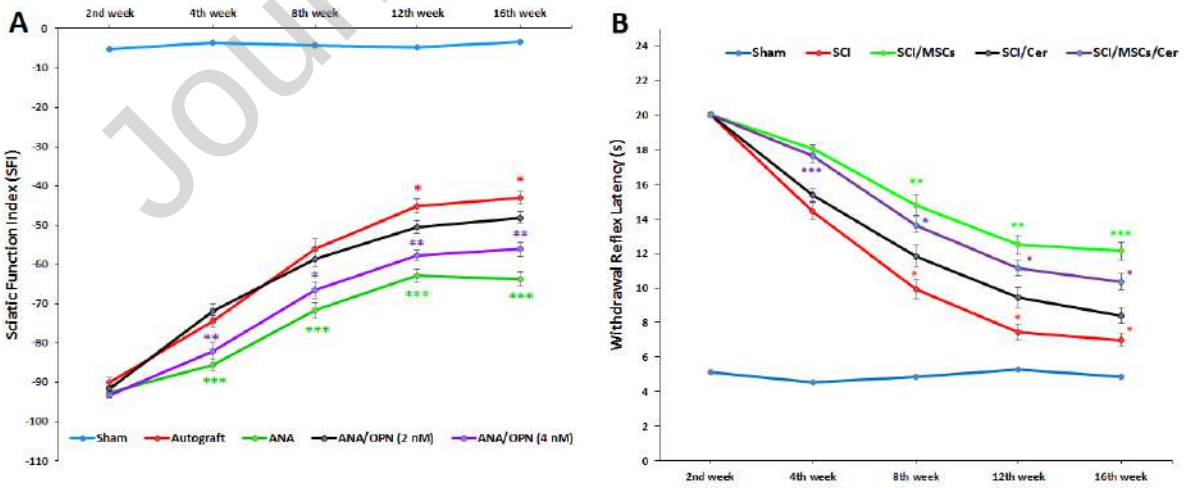

Figure 1. Assessment of sensorimotor behavior. (A) The motor function was evaluated using the sciatic function index (SFI). (B) Thermal pain threshold assessed by the thermal paw withdrawal

reflex latency (PWRL). Assessments were conducted pre-surgery and 2nd, 4th, 8th, 12th, and 16th weeks post-surgery. One-way analysis of variance and Tukey's post-hoc tests were used to analyze data. The data is expressed as mean ± standard error of the mean (SEM) (n = 10). * P < 0.05, ** P < 0.01, and *** P < 0.001 indicate significance compared to the nerve ANA/OPN (2 nM) group.

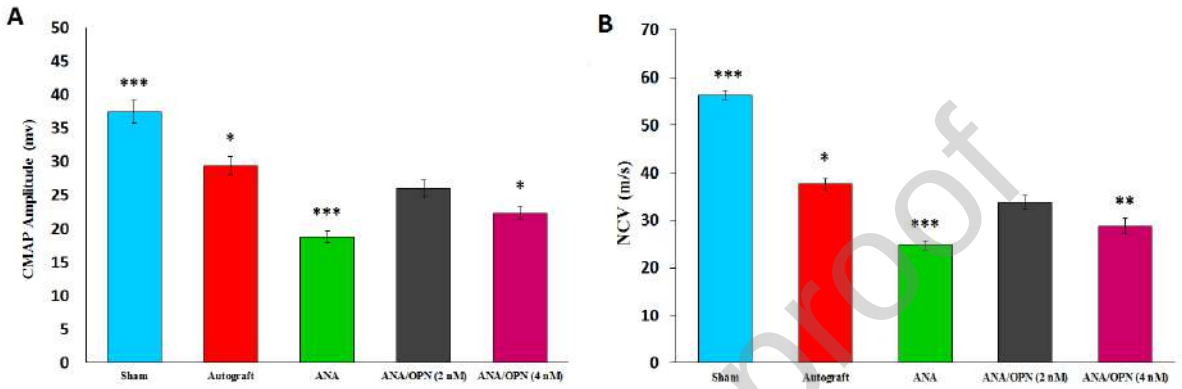

Figure 2. Electrophysiological assessments. The compound muscle action potential (CMAP) and nerve conduction velocity (NCV) were evaluated 16 weeks post-surgery. The CMAP amplitude (A) and NCV (B) were recorded at the gastrocnemius muscle of the operated side in each group after proximal stimulation. One-way analysis of variance and Tukey's post-hoc tests were used to analyze data. The data is expressed as mean ± standard error of the mean (SEM) (n = 10). * P < 0.05, ** P < 0.01, and *** P < 0.001 indicate significance compared to the nerve ANA/OPN (2 nM) group.

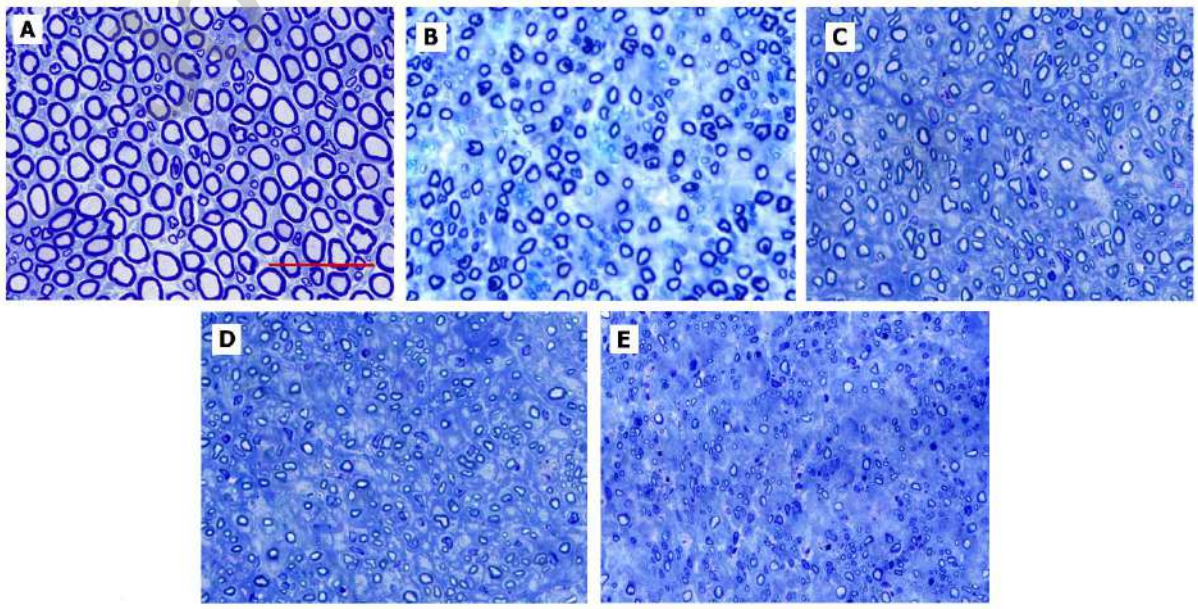

Figure 3. Toluidine blue staining of regenerated sciatic nerves distal to the lesion site at the 16th postoperative week. (A) the Sham group, (B) the autograft group, (C) the ANA group, (D) the ANA/OPN (2 nM) group, and (E) the ANA/OPN (4 nM) group. (Scale bar: 100 μm).

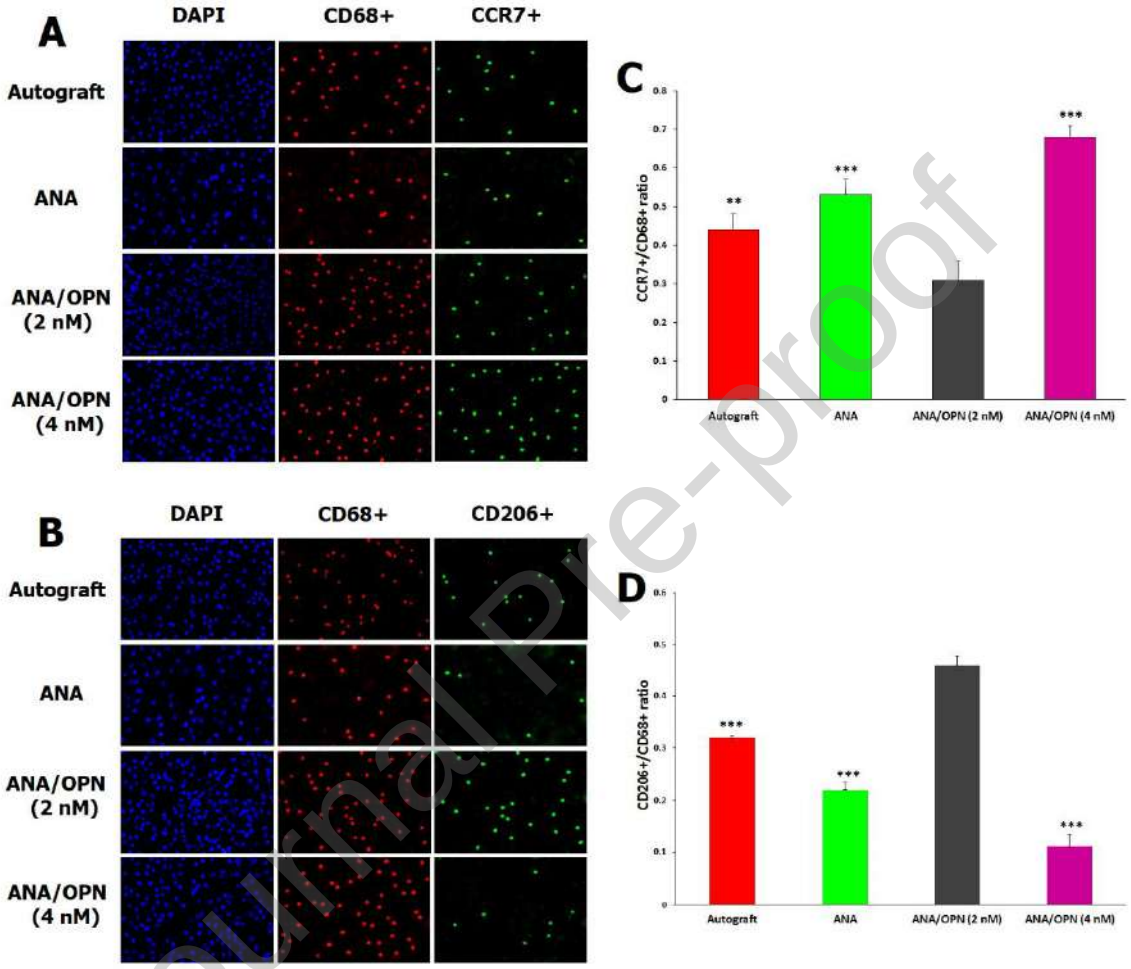

Figure 4. Characterization of macrophages in injured sciatic nerves was conducted. (A) Double immunofluorescent staining depicted [(CD68+ (red)/CCR7+ (green)] macrophages (M1). Negative control staining without the primary antibody (Secondary antibody alone) showed no detectable macrophage markers labeling. (B) Immunofluorescent staining of [(CD68+ (red)/CD206+ (green)] macrophages (M2) was also performed, with negative control staining (Secondary antibody alone) showing negative results. Scale bar (50 μm). (C) Quantitative assessment of the CCR7+/CD68+ ratio. (D) The CD206+/CD68+ ratio. One-way analysis of variance and Tukey's post-hoc tests were used to

analyze data. The data is expressed as mean ± standard error of the mean (SEM) (n = 10). * P < 0.05, ** P < 0.01, and *** P < 0.001 indicate significance compared to the nerve ANA/OPN (2 nM) group.

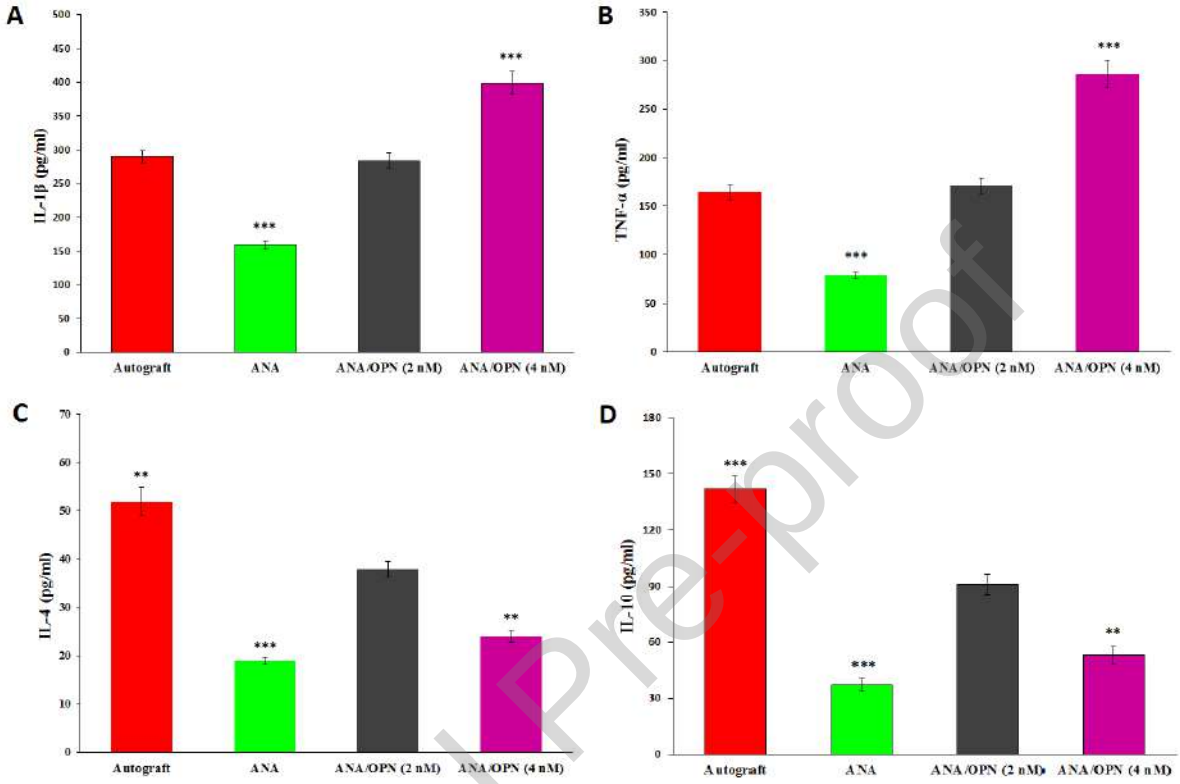

Figure 5. ELISA evaluation of pro-inflammatory cytokines and anti-inflammatory cytokines three weeks after surgery in nerve grafts. (A) IL-1β, (B) TNF-α, (C) IL-4, and (D) IL-10. One-way analysis of variance and Tukey's post-hoc tests were used to analyze data. The data is expressed as mean ± standard error of the mean (SEM) (n = 10). * P < 0.05, ** P < 0.01, and *** P < 0.001 indicate significance compared to the nerve ANA/OPN (2 nM) group.

Table 1. Histomorphometric assessment of myelinated axons in cross-sections of regenerated sciatic nerves 16 weeks post-surgery. Results are presented as mean ± SEM (n = 10). * P < 0.05, ** P < 0.01, and *** P < 0.001 indicate significance compared to the autograft group. # P < 0.05, ## P < 0.01, and ### P < 0.001 indicate significance compared to the ANA/OPN (2 nM) group.

	Myelinated Fiber Count	Myelinated Fiber Diameter (µm)	Myelin Sheath Thickness (µm)	G-Ratio
Sham	642± 6873 *** ###	0.67±7.37 *** ###	0.17± 1.15 *** ###	0.68 ** ##
Autograft	5018 ± 817	0.46± 5.22	0.12± 0.69	0.73
ANA	437 ±3061 *** ###	0.42± 3.57 *** ###	0.0.07± 0.32 *** ###	0.82 *** #
ANA/OPN (2 nM)	685 ±4228.5 *	0.59±4.65 *	0.12±0.57 *	0.75 –
ANA/OPN (4 nM)	472 ± 3575 *** #	0.54 ±4.06 *** #	0.43 ± 0.14 *** #	0.79 *** –

Author Statement

S. W and A. A conceived and designed the evaluation and drafted the manuscript. S. Z, L.S, T.K, participated in designing the evaluation, performed parts of the statistical analysis, and helped to draft the manuscript. Z. O, A. F, M.H and M. G. re-evaluated the clinical data, revised the manuscript and performed the statistical analysis, and revised the manuscript. All authors read and approved the final manuscript.

Highlights

- Inflammation is vital for nerve regeneration it eliminates growth-inhibiting components and creates a supportive environment for axonal regrowth. Therefore, regulating the inflammatory response seems to be a suitable strategy for improving nerve.
- Macrophages are essential for peripheral nerve regeneration and play a crucial role in the immune response and tissue repair following nerve injury.
- Osteopontin is a multifunctional glycoprotein with both pro-inflammatory and anti-inflammatory properties. This dual functionality of osteopontin highlights its complex role in immune response modulation.
- Osteopontin addition to decellularized nerves improves the scaffold's regenerative capabilities by modulating the immune response and facilitating the regeneration of axons.